PERGAMON

International Journal of Solids and Structures 38 (2001) 4477–4488

INTERNATIONAL JOURNAL OF SOLIDS and STRUCTURES

www.elsevier.com/locate/ijsolstr

A contact mechanism based theory of Maxwell matrix composites

Han Zhu *

Department of Civil and Environmental Engineering, Arizona State University, Tempe, AZ 85287-5306, USA

Received 23 April 1999; in revised form 20 April 2000

Abstract

Using the binder-contact laws in deriving the stress–strain relations for a composite with elastic particles/inclusions/fibers and a Maxwell type of viscoelastic matrix/binder is presented in this article. This derivation is physically based and it establishes a functional correlation of how the viscosity at the binder/matrix level is blended into that at the composite level. The derived viscoelastic stress–strain equations are multiaxial, and their equivalent models are analyzed for three scenarios. A confined creep simulation is also given with its predications being compared with the experimental results. © 2001 Elsevier Science Ltd. All rights reserved.

Keywords: Composite materials; Visco-elastic matrix; Maxwell model; Contact laws; Fabric tensor; Stress; Strain; Creep; Asphalt concrete

1. Introduction

Constitutive analysis of the composites that comprise elastic particles/inclusion/fibers and a viscous matrix/binder is an important subject, because those composites assemble many realistic engineering materials. The methods in analyzing those composites can be found in a number of published studies. A well-known method is an elastic analogy that follows the so-called ''corresponding theory'', in which the viscoelastic stress–strain analysis can be carried out in the Laplace domain and be treated as if it follows the elasticity theory. The inverse Laplace transform then can be applied to the Laplace stress and strain quantities to obtain the real time domain solutions. The early work following this approach can be found in Schapery (1974), and Scherer and Rekhson (1982). Hashin (1983) gave an overview in this area prior to 1983. Another way to simulate the viscous significance is to employ the potential theory or Eshelby's principle that are modified to include the viscous effect (Castaneda and Willis, 1988; Chen and Cheng, 1997). Since the Laplace transform or potential theory usually requires a lengthy mathematical manipulation, an engineering approach can be adopted in estimating the matrix viscous response by adding a

* Tel.: +1-602-965-2745; fax: +1-602-965-0557.
E-mail address: han.zhu@asu.edu (H. Zhu).

PII: S0020-7683(00)00288-2

viscous term to the "regular" elastic stress–strain equations, as shown in the work of Zabaras and Pervez (1990) on the viscous damping approximation of laminated plates. This type of approach is mostly implemented in conjunction with a numerical method like FEM.

In this article, a contact mechanism based theory is presented in deriving the stress–strain relationship for a viscous matrix composite. Here, the contact mechanism is the force–displacement interaction of particle–particle contact (contact laws) that serves as the vehicle that transforms micro stress/strain variables to macro stress/strain variables defined in a particle assembly. Due to the discrete feature of a particle assembly, the local stress field is easily defined by using the theorem of stress means. Two type of variables then are introduced. One is the "branches", which are vectors connecting the centroids of contacting particles. The other is the variables that characterize the statistical natures of particle packing such as coordination number, and other distribution configurations. Subsequently, the strain field can be defined in conjunction with those types of variables and the stress–strain equations can then be established.

Earlier work in this area can be found in soil and particulate mechanics in dealing with a particle assembly. Finney (1970) and Shahinpoor (1981) employed the "Voronoi Polyhedra" in describing the behaviors of a granular medium. Jenkins (1987) and Bathurst and Rothenburg (1988) derived the stress–strain relationships in the framework of a microstructural continuum approach. Satake (1982), Oda et al. (1982), Kanatani (1984) and Cowin (1985) introduced the concept of "fabric tensor" to accommodate the statistical nature of particle packing. Chang et al. (1990) characterized the skeleton of a particle assembly by using a density distribution function of inter-particle contacts.

The study of contact laws itself is an active subject. The most known case in this subject is the Hertz contact problem (Johnson, 1989). A good collection can be found in the book of Johnson (1989) and Gladwell (1980). Recently, Zhu et al. (1996a,b and 1997a) derived the closed-form contact laws for a system of two-particle bound with a Maxwell or Voigt type of viscoelastic binder for three modes: compressive, tangential and rolling. Those Maxwell contact laws will be used later in this study to formulate the stress–strain equations.

With the presence of a Maxwell matrix/binder, now the material can be regarded as a composite of a "coated" particle assembly. The modification is made in this article by replacing the particle–particle (or particle–binder(elastic)–particle) contact laws with those of particle–binder (Maxwell)–particle laws on the basis of the early work in the soil and particulate mechanics cited above. The viscous nature of the binder/matrix then erects its effect on the stress–strain derivation through the incorporation of those binder-contact laws. This is the major work of this article. In addition, it contains a model analysis that demonstrates the equivalent viscoelastic behavior in responding to a Maxwell binder composite. A creep simulation of asphalt concrete is then presented, and its predictions are compared with the corresponding experimental results.

2. Dry particle results

Based on the work of those researchers (Christoffersion et al., 1981; Rothenberg and Selvafurai, 1981; and Chang et al., 1996; etc.), the volume averaged stress field σ_{ij} defined in a granular medium V of dry particles can be formulated by

$$\sigma_{ij} = \frac{1}{V}\sum_{m=1}^{M} L_i(x^m) f_j(x^m), \quad x^m \in V, \tag{2.1}$$

where $L_i(x^m)$ is the branch vector and $f_j(x^m)$ represents the inter-particle contact forces at the contact point x^m within the space V in the global coordinate system. M is the total number of contacts and $\sum$ denotes a summation over all contact points x^m (Fig. 1).

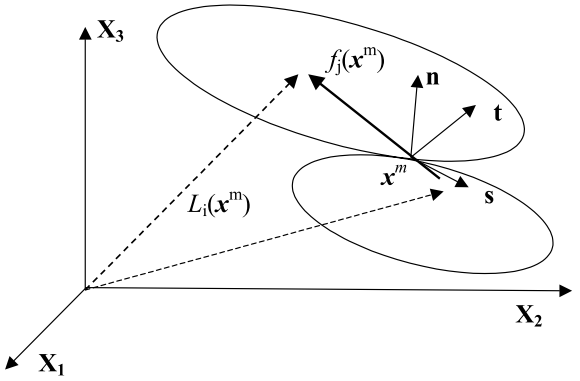

Fig. 1. Sketch of the coordinates (n, s, t), contact point x^m, the contact forces $f_i(x^m)$ and the branch vector $L_j(x^m)$.

The contact laws then are introduced, which relate the discrete contact forces $f_j(x^m)$ in a local coordinate system $(n_j(x^m),\ s_j(x^m),\ t_j(x^m))$ with the corresponding displacement components $\delta_j(x^m)$ (or relative approaches as termed in the contact mechanics) also in the local coordinate system $(n_j(x^m),\ s_j(x^m),\ t_j(x^m))$:

$$\begin{aligned} f_n(x^m) &= K_n(x^m)\delta_n(x^m), \\ f_s(x^m) &= K_s(x^m)\delta_s(x^m), \\ f_t(x^m) &= K_t(x^m)\delta_t(x^m), \end{aligned} \tag{2.2}$$

where $K_n(x^m)$, $K_s(x^m)$ and $K_t(x^m)$ are the normal, first tangential and second tangential contact stiffness coefficients at x^m. The $(n_j(x^m), s_j(x^m), t_j(x^m))$ coordinates are placed at the contact point x^m (Fig. 1). $n_j(x^m)$ is the unit vector normal to the contact surface at the contact point x^m, $s_j(x^m)$ and $t_j(x^m)$ are two unit vectors perpendicular to each other as well as to $n_j(x^m)$.

Assuming a uniform strain field, the branch vectors $L_j(x^m)$ can be further related to ε_{ij}, the volume averaged strain field, by the following relation:

$$\delta_i(x^m) = L_j(x^m)\varepsilon_{ij}, \tag{2.3}$$

and consolidating Eqs. (2.1)–(2.3) yields the stress–strain equations for the particle assembly with an appropriate coordinate transform scheme (Chang and Misra, 1990):

$$\begin{aligned} \sigma_{ij} &= \left\{ \frac{1}{V}\sum_{m=1}^{M} L_i(x^m)K_{jl}(x^m)L_k(x^m) \right\}\varepsilon_{kl}, \\ K_{jl}(x^m) &= K_n(x^m)n_j(x^m)n_l(x^m) + K_s(x^m)s_j(x^m)s_l(x^m) + K_t(x^m)t_j(x^m)t_l(x^m). \end{aligned} \tag{2.4}$$

Eq. (2.4) represents the result of the averaged stress–strain relationship defined in a particle assembly and derived on the contact mechanism based homogenization process.

3. Maxwell binder effect

The contact laws given in Eq. (2.2) are valid for describing the force-deformation relation of a system of two elastic particles bound with an elastic binder. The presence of a Maxwell binder in the particle assembly requires a modification of those contact laws to accommodate the viscoelastic effect. Following the work of

Zhut et al. (1996a,b), the contact laws for a system of two particles bound with a Maxwell binder now become time dependent, and have the following representations:

$$\begin{aligned} f_n(x^m) &= K_n(x^m)\delta_n(x^m) - \int_0^t K_n\lambda_n \mathrm{e}^{-\lambda_n(x^m)(t-\tau)}\delta_n(x^m)\,\mathrm{d}\tau, \\ f_s(x^m) &= K_s(x^m)\delta_s(x^m) - \int_0^t K_s\lambda_s \mathrm{e}^{-\lambda_s(x^m)(t-\tau)}\delta_s(x^m)\,\mathrm{d}\tau, \\ f_t(x^m) &= K_t(x^m)\delta_t(x^m) - \int_0^t K_t\lambda_t \mathrm{e}^{-\lambda_t(x^m)(t-\tau)}\delta_t(x^m)\,\mathrm{d}\tau, \end{aligned} \tag{3.1}$$

where the scale parameter t is the time variable. $\lambda_n(x^m)$, $\lambda_s(x^m)$ and $\lambda_t(x^m)$ are inverse to what is the so-called time retardation parameters, which depend on the viscosity and spring constants of the Maxwell model, and their definitions can also be found in Zhu et al. (1996a,b).

Replacing Eq. (2.2) with Eq. (3.1) and repeating the steps given in the Section 2, the stress–strain relations for a particle assembly bound by a Maxwell binder are obtained:

$$\sigma_{ij}(t) = \left\{ \frac{1}{V}\sum_{m=1}^{M} L_i(x^m)K_{jl}(x^m)L_k(x^m) \right\}\varepsilon_{kl} - \int_0^t \left\{ \frac{1}{V}\sum_{m=1}^{M} L_i\left(x^m,t'\right)K^*_{jl}\left(x^m,t,t'\right)L_k\left(x^m,t'\right) \right\}\varepsilon_{kl}(t')\,\mathrm{d}t', \tag{3.2}$$

where $K_{jl}(x^m)$ is defined in Eq. (2.4), and

$$\begin{aligned} K^*_{jl}\left(x^m,t,t'\right) = {} & K_n\left(x^m,t'\right)n_j(x^m)n_l(x^m)\lambda_n(x^m)\mathrm{e}^{-\lambda_n(x^m)(t-t')} + K_s\left(x^m,t'\right)s_j(x^m)s_l(x^m)\lambda_s(x^m)\mathrm{e}^{-\lambda_s(x^m)(t-t')} \\ & + K_t\left(x^m,t'\right)t_j(x^m)t_l(x^m)\lambda_t(x^m)\mathrm{e}^{-\lambda_t(x^m)(t-t')}. \end{aligned} \tag{3.3}$$

Eq. (3.2) is of the type of Volterra equations of the second kind. It is easily observed that, when the integral portion of the right-hand side of Eq. (3.2) vanishes, Eqs. (3.2) and (2.4) become identical. This means that the effect of Maxwell binder viscosity is solely represented by the integral portions of the equation. The differential representation for Eq. (3.2) is also available, but it is much lengthy in comparison with Eq. (3.2).

The derived stress–strain relations given in Eq. (3.2) are unrefined. Many levels of simplification are available based on the introduction of characteristic distributions like those of the particle location, size gradation and angularity, the coordination number, etc. Those distributions will determine the effective moduli and the anisotropic characteristics of the composite. Following the work of Chang and Ma (1992) on the dry particle assembly, an isotropic stress–strain relation can be derived:

$$\begin{aligned} \sigma_{ij}(t) = {} & 4\alpha K_n\delta_{ij}\left[\varepsilon_{kk}(t) - \int_0^t \lambda_n \mathrm{e}^{-\lambda_n(t-t')}\varepsilon_{kk}(t')\,\mathrm{d}t'\right] - 4\alpha K_s\delta_{ij}\left[\varepsilon_{kk}(t) - \int_0^t \lambda_s \mathrm{e}^{-\lambda_s(t-t')}\varepsilon_{kk}(t')\,\mathrm{d}t'\right] \\ & + 8\alpha K_n\left[\varepsilon_{ij}(t) - \int_0^t \lambda_n \mathrm{e}^{-\lambda_n(t-t')}\varepsilon_{ij}(t')\,\mathrm{d}t'\right] + 12\alpha K_s\left[\varepsilon_{ij}(t) - \int_0^t \lambda_s \mathrm{e}^{-\lambda_s(t-t')}\varepsilon_{ij}(t')\,\mathrm{d}t'\right], \end{aligned} \tag{3.4}$$

where α is defined as (Chang and Ma, 1992)

$$\alpha = \frac{MR^2}{30V}, \tag{3.5}$$

and δ_{ij} is Kronecker delta, the subscript k is the dummy index, K_n and K_s represent the averaged normal and tangential contact stiffness coefficients, respectively. λ_n and λ_s represent the averaged normal and tangential time retardation parameters, respectively. R is the averaged characteristic dimension of the particles. α can further be interpreted as (Chang et al., 1990)

$$\alpha = \frac{N_c}{40\pi R(1+e)}, \tag{3.6}$$

where e is the air void ratio and N_c is the averaged coordination number.

4. Model analysis I

Eq. (3.2) denotes the stress–strain relationships for a particle assembly bound with a Maxwell binder. Naturally, the question rises as to what is the equivalent viscoelastic model responding to Eq. (3.2). For answering this question, an uniaxial model analysis is given in this section.

By setting all the stress and strain components to zero except σ_{11} (now denoted by σ) and ε_{11} (now denoted by ε) in Eq. (3.2), we obtain an uniaxial σ–ε equation:

$$\begin{aligned}
&\sigma(t) = \sum_{m=1}^{M}[I_{n,m} + I_{s,m} + I_{t,m}],\\
&I_{n,m} = K_{n,m}\left[\varepsilon(t) - \int_0^t \lambda_{n,m} e^{-\lambda_{n,m}(t-\tau)}\varepsilon(\tau)d\tau\right],\\
&I_{s,m} = K_{s,m}\left[\varepsilon(t) - \int_0^t \lambda_{s,m} e^{-\lambda_{s,m}(t-\tau)}\varepsilon(\tau)d\tau\right],\\
&I_{t,m} = K_{t,m}\left[\varepsilon(t) - \int_0^t \lambda_{t,m} e^{-\lambda_{t,m}(t-\tau)}\varepsilon(\tau)d\tau\right],
\end{aligned} \tag{4.1}$$

where

$$\begin{aligned}
&K_{n,m} = \frac{L_1^2(x^m)n_1^2(x^m)K_n(x^m)}{V},\\
&K_{s,m} = \frac{L_1^2(x^m)s_1^2(x^m)K_s(x^m)}{V},\\
&K_{t,m} = \frac{L_1^2(x^m)t_1^2(x^m)K_t(x^m)}{V},\\
&\lambda_{n,m} = \lambda_n(x^m), \qquad \lambda_{s,m} = \lambda_s(x^m), \qquad \lambda_{t,m} = \lambda_t(x^m).
\end{aligned} \tag{4.2}$$

It can easily be verified that, based on the theory of classic viscoelasticity, the equivalent viscoelastic model equation (4.1) represents a generalized Maxwell model with $3M$ units (Fig. 2).

Next, we apply the Laplace transform to Eq. (4.1), and it yields

$$\bar{\varepsilon}(p) = \left[\sum_{m=1}^{M}\left(\frac{K_{n,m}}{p+\lambda_{n,m}} + \frac{K_{s,m}}{p+\lambda_{s,m}} + \frac{K_{t,m}}{p+\lambda_{t,m}}\right)\right]^{-1}\frac{\bar{\sigma}(p)}{p}, \tag{4.3}$$

where $\bar{\sigma}(p)$ and $\bar{\varepsilon}(p)$ are the strain and stress defined in the Laplace domain.

Based on a lemma given in the book of Bland (1960), the following identity can be proclaimed:

$$\begin{aligned}
&\left[\sum_{m=1}^{M}\left(\frac{K_{n,m}}{p+\lambda_{n,m}} + \frac{K_{s,m}}{p+\lambda_{s,m}} + \frac{K_{t,m}}{p+\lambda_{t,m}}\right)\right]^{-1} = \frac{p}{K_c} + \frac{1}{\eta_c} + \sum_{m=1}^{3M-1}\frac{p}{\eta_m(p+\lambda_m)},\\
&K_c = \sum_{m=1}^{M}(K_{n,m} + K_{s,m} + K_{t,m}), \qquad \eta_c = \sum_{m=1}^{M}\left(\frac{K_{n,m}}{\lambda_{n,m}} + \frac{K_{s,m}}{\lambda_{s,m}} + \frac{K_{t,m}}{\lambda_{t,m}}\right),
\end{aligned} \tag{4.4}$$

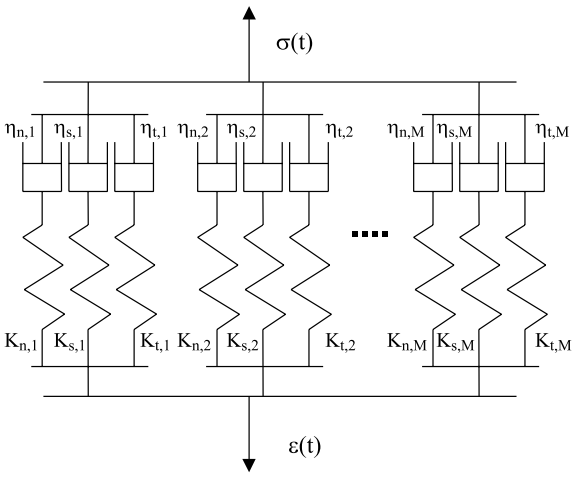

Fig. 2. Generalized Maxwell model with $3M$ units.

where, η_m and λ_m, $m = 1, 2, \ldots, (3M-1)$, are all positive, and they depend on $K_{n,m}$, $K_{s,m}$, $K_{t,m}$, $\lambda_{n,m}$, $\lambda_{s,m}$ and $\lambda_{t,m}$, $m = 1, 2, \ldots, M$.

It needs to point that since K_c and η_c defined in Eq. (4.4) are as the summation over the coefficients of contact stiffness and viscosity at each and every contact point x^m in all three directions with a V sitting in the denominator (Eq. (4.2)), they are a volume averaged quantity. This will be further discussed later in this article.

With the help of Eq. (4.3), the inverse Laplace transform to Eq. (4.4) is readily available, and it reads

$$\varepsilon(t) = \frac{\sigma(t)}{K_c} + \int_0^t \frac{\sigma(\tau)\mathrm{d}\tau}{\eta_c} + \sum_{m=1}^{3M-1} \frac{1}{\eta_m} \int_0^t \mathrm{e}^{-\lambda_m(t-\tau)}\sigma(\tau)\,\mathrm{d}\tau. \tag{4.5}$$

Clearly, the stress–strain equation given in Eq. (4.5) indicates that its corresponding viscoelastic model is a generalized Voigt model (Fig. 3), which is equivalent to the generalized Maxwell model given in Fig. 2.

The above analysis is also valid for the case of $\sigma_{12}(t)$–$\varepsilon_{12}(t)$, $\sigma_{22}(t)$–$\varepsilon_{22}(t)$, $\sigma_{13}(t)$–$\varepsilon_{13}(t)$, $\sigma_{23}(t)$–$\varepsilon_{23}(t)$, and $\sigma_{33}(t)$–$\varepsilon_{33}(t)$, and the same conclusion can be drawn with regard to the type of viscoelastic model among the paired stresses and strains.

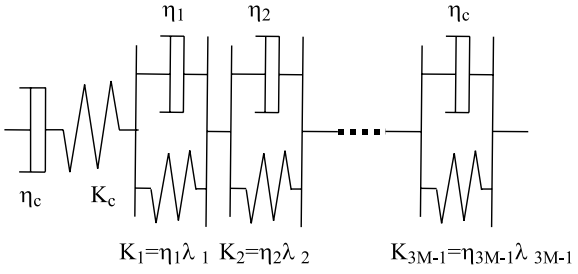

Fig. 3. Generalized Voigt model.

5. Model analysis II

A model analysis to Eq. (3.4) is conducted in this section. Again, by letting all stress and strain components vanish except one normal stress, denoted by σ, and one normal strain, denoted by ε, Eq. (3.4) now reads

$$\sigma(t) = 12\alpha K_n\left[\varepsilon(t) - \int_0^t \lambda_n e^{-\lambda_n(t-t')}\varepsilon(t')\,dt'\right] + 8\alpha K_s\left[\varepsilon(t) - \int_0^t \lambda_s e^{-\lambda_{sn}(t-t')}\varepsilon(t')\,dt'\right], \tag{5.1}$$

and in the Laplace domain, Eq. (5.1) has the following expression:

$$\bar{\varepsilon}(p) = \left(\frac{12\alpha K_n}{p+\lambda_n} + \frac{8\alpha K_s}{p+\lambda_s}\right)^{-1}\frac{\bar{\sigma}(p)}{p} = \left(\frac{1}{K_n'+K_s'} + \frac{1}{p(\eta_n'+\eta_s')} + \frac{(\lambda_n-\lambda')(\lambda'-\lambda_s)}{\lambda'(K_n'+K_s')(p+\lambda')}\right)\bar{\sigma}(p), \tag{5.2}$$

where

$$\lambda' = \frac{\lambda_n K_s' + \lambda_s K_n'}{K_s'+K_n'}, \quad K_n' = 12\alpha K_n, \quad K_s' = 8\alpha K_s, \quad \eta_n' = \frac{K_n'}{\lambda_n}, \quad \eta_s' = \frac{K_s'}{\lambda_s}. \tag{5.3}$$

Again, the time domain expression for Eq. (5.2) can be obtained by using the method of inverse Laplace transform:

$$\varepsilon(t) = \frac{\sigma(t)}{K_n'+K_s'} + \int_0^t \frac{\sigma(\tau)d\tau}{\eta_n'+\eta_s'} + \frac{(\lambda_n-\lambda')(\lambda'-\lambda_s)}{\lambda'(K_n'+K_s')}\int_0^t e^{-\lambda'(t-\tau)}\sigma(\tau)\,d\tau. \tag{5.4}$$

It can easily be seen that Eq. (5.4) viscoelastically responds to what a four-element model does (Fig. 4).

In addition to the normal stress–strain case, by an analogy, the model analysis can also be extended to the shear stress–strain case, and the conclusion with regard to the model representation remains the same for both normal and shear cases.

6. Model analysis III

Two uniaxial model analyses are given in the previous sections. In this section, based on Eq. (3.4), a two-dimensional modeling will be pursued on an axially symmetric representation. Assuming an uniform stress–strain state, the non-vanishing components are (σ_z, σ_r and σ_θ) and (ε_z, ε_r and ε_θ) with the conditions that $\sigma_r = \sigma_\theta$ and $\varepsilon_r = \varepsilon_\theta$, Eq. (3.4) in cylindrical coordinates (r, z, θ) now becomes

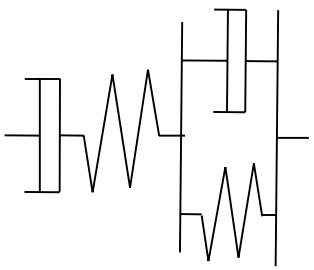

Fig. 4. Four-element model.

$$\sigma_z(t) = 12\alpha K_n\left[\varepsilon_z(t) - \int_0^t \lambda_n e^{-\lambda_n(t-t')}\varepsilon_z(t')dt'\right] + 8\alpha K_s\left[\varepsilon_z(t) - \int_0^t \lambda_s e^{-\lambda_{sn}(t-t')}\varepsilon_z(t')dt'\right] + 8\alpha K_n\left[\varepsilon_r(t) - \int_0^t \lambda_n e^{-\lambda_n(t-t')}\varepsilon_r(t')dt'\right] - 8\alpha K_s\left[\varepsilon_r(t) - \int_0^t \lambda_s e^{-\lambda_{sn}(t-t')}\varepsilon_r(t')dt'\right], \tag{6.1}$$

$$\sigma_r(t) = 4\alpha K_n\left[\varepsilon_z(t) - \int_0^t \lambda_n e^{-\lambda_n(t-t')}\varepsilon_z(t')dt'\right] - 4\alpha K_s\left[\varepsilon_z(t) - \int_0^t \lambda_s e^{-\lambda_{sn}(t-t')}\varepsilon_z(t')dt'\right] + 16\alpha K_n\left[\varepsilon_r(t) - \int_0^t \lambda_n e^{-\lambda_n(t-t')}\varepsilon_r(t')dt'\right] + 4\alpha K_s\left[\varepsilon_r(t) - \int_0^t \lambda_s e^{-\lambda_{sn}(t-t')}\varepsilon_r(t')dt'\right]. \tag{6.2}$$

Eq. (6.1) presents a 2-axial viscoelastic behavior. Fig. 5 shows an attempt to graphically depict an equivalent 2-axial model of Eq. (6.1). Though with a ε_r-axial Maxwell unit sitting on the stress side, which characterizes the reaction to the imposed lateral radius stress (Poisson's effect), the equivalent model may still be called a two-axial generalized Maxwell model since the inequality, $K_n > K_s$, is always valid (Zhu et al., 1996a).

Eqs. (6.1) and (6.2) are referred as the relaxation model. The corresponding creep model is also available by applying the Laplace transform technique to Eqs. (6.1) and (6.2). After a lengthy manipulation, the creep model of Eqs. (6.1) and (6.2) is obtained as

$$\varepsilon_v(t) = \varepsilon_z(t) + 2\varepsilon_r(t) = \frac{\sigma_z(t) + 2\sigma_r(t)}{2.5K_n^*} + \int_0^t \frac{[\sigma_z(\tau) + 2\sigma_r(\tau)]\lambda_n d\tau}{2.5K_n^*}, \tag{6.3}$$

$$\varepsilon_z(t) = \frac{0.8\sigma_z(t) - 0.4\sigma_r(t)}{K_n^* + K_s^*} + \int_0^t \frac{[0.8\sigma_z(\tau) - 0.4\sigma_r(\tau)]\lambda_n\lambda_s d\tau}{(K_n^* + K_s^*)\lambda^*} - \int_0^t \frac{[0.8\sigma_z(\tau) - 0.4\sigma_r(\tau)](\lambda_n - \lambda^*)(\lambda_s - \lambda^*)_s e^{-\lambda^*(t-\tau)}d\tau}{(K_n^* + K_s^*)\lambda^*} + \frac{2K_s^*[\sigma_z(t) + 2\sigma_r(t)]}{15K_n^*(K_n^* + K_s^*)} + \int_0^t \frac{2K_s^*[\sigma_z(\tau) + 2\sigma_r(\tau)]\lambda_n^2 d\tau}{15K_n^*(K_n^* + K_s^*)\lambda^*} - \int_0^t \frac{2K_s^*[\sigma_z(\tau) + 2\sigma_r(\tau)](\lambda - \lambda^*)_n^2 e^{-\lambda^*(t-\tau)}d\tau}{15K_n^*(K_n^* + K_s^*)\lambda^*}, \tag{6.4}$$

where $\varepsilon_v(t)$ in Eq. (6.3) is the volumetric strain (the first strain invariant), and

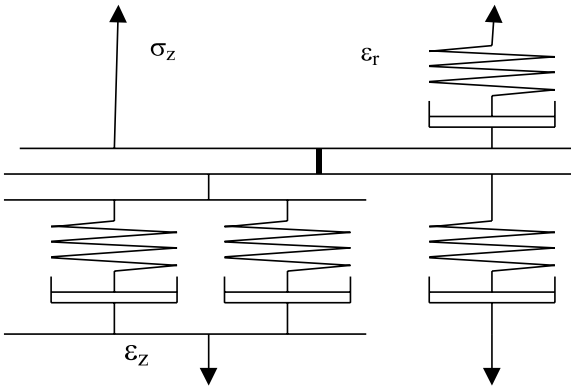

Fig. 5. Two-dimensional equivalent visco-elastic model.

$$K_n^* = 8\alpha K_n, \qquad K_s^* = 12\alpha K_s, \qquad \lambda^* = \frac{K_s^*\lambda_s + K_s^*\lambda_n}{K_n^* + K_s^*}. \tag{6.5}$$

One important laboratory evaluation of asphalt concrete quality is to conduct confined or unconfined creep tests on the cylindrical specimens of hot mix asphalt (HMA). Based on his experimental work, Monismith et al. (1994) indicates that asphalt pavement with good quality exhibits isotropic responses. Whereby, Eqs. (6.3) and (6.4) may be used to simulate HMA creep tests. A creep example is implemented following the input and testing results reported by Brown and Cooper (1980). The sample dimension is a cylinder of 6 in. in diameter and 12 in. in height. The applied axial and lateral compressive pressures are 0.267 and 0.167 MPa, respectively. Two quantities ε_v (volumetric strain and defined in Eq. (6.3)) and ε_s (shear strain) are computed. Where ε_s is defined as

$$\varepsilon_s = \tfrac{1}{3}(3\varepsilon_z - \varepsilon_v). \tag{6.6}$$

K_n, K_s, λ_n and λ_s shown in Eqs. (6.3) and (6.4) are specified in the work of Zhu et al. (1996a,b). Those parameters along with α are related to the physical and geometric properties of asphalt and aggregates with the input as follows:

averaged aggregate size $S = 5.682$ mm ($R = 2.841$ mm).
averaged contact radius $a = k \times R$ ($k = 0.1$ at $t = 0$),
averaged thickness of asphalt binder $h_0 = 0.075$ mm at $t = 0$ (Lee and Dass, 1993).
Young's modulus of aggregates $E_p = 27.56$ GPa (4×10^6 psi) (Trefethen, 1959),
shear modulus of asphalt binder $G_b = 0.1$ GPa (Lewandowski et al., 1992).
Poisson's ratio for aggregates = 0.15,
coordination number $N_c = 7.0$ (Lee and Dass, 1993).
VTM = 0.05,
binder viscosity constant = 1.0 GPa s (Hopman et al., 1992).

A discretization scheme is employed with respect to the time variable t, and the creep responses are computed. The details of the scheme can be found in the report by Zhu and Dass (1996). Those numerical responses then are plotted in Figs. 6 and 7 along with the experimental results reported by Brown and Cooper (1980).

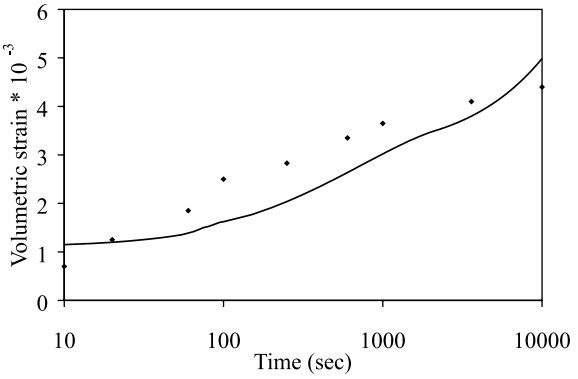

Fig. 6. Volumetric strain versus time. The solid line represents the simulation result, and the symbols are based on the test results reported by Brown and Cooper (1980).

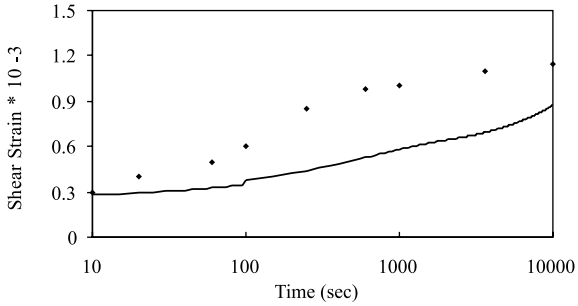

Fig. 7. Shear strain versus time. The solid line represents the simulation result and the symbols are based on the test results reported by Brown and Cooper (1980).

Figs. 6 and 7 show that the model equation (6.4) can fairly capture the creep behavior of asphalt concrete, though it appears that this model may be considered as the first step in developing more robust analytical simulations (Zhu, 1998).

7. Discussions

This article presents a contact mechanism based constitutive theory in which, the binder contact laws play a critic role in transforming the characteristic of Maxwell type of viscoelasticity at the binder/matrix level to that at the composite level in a parallel manner. The transform is pursued in a fashion that preserves a clear physical rationale and requires, in comparison with the integral transform method, straightforward and less cumbersome mathematical manipulations. A Maxwell type of binder results in a Maxwell type of the composite as Eq. (4.1) and Fig. 2 indicate.

The model analysis provides an insight of how the stress filed, σ_{ij}, and the strain field, ε_{ij}, are related functionally. Here, σ_{ij} and ε_{ij} are defined as a volume averaged quantity. The first-order approximation on the relation between σ_{ij} and ε_{ij} in an uniaxial case is actually governed by a single Maxwell element as shown in Eq. (4.5) with the elastic and viscosity constants being K_c and η_c, respectively. K_c and η_c are defined in Eqs. (4.2) and (4.4) and are computed by the summation of contact stiffness and viscosity over all contact points x^m in V, whereby they are also volume averaged quantities. This indicates that the volume averaged physical and geometric properties of a composite delegate the defining of the volume averaged stress–strain relation, and the delegation assures that using the averaged stress and strain fields to describe the mechanical behavior of a composite is both feasible and physically consistent.

When particles/fibers/inclusions are elastic and the matrix/binder follows a Maxwell type of viscoelasticity, it appears intuitive that the composite may behave like a viscoelastic solid that can be represented by generalized Maxwell model as given in Fig. 2. But the issue is that how many Maxwell units are needed at the composite level. The model analysis provides an understanding regarding this issue. It shows that depending on the simplification level appropriate for a specific problem, the simplest one is a four-element model as given in Fig. 4. In addition, both Figs. 3 and 4 contain one Maxwell unit, which characterized the volume averaged correspondence between the volume averaged stress and volume averaged strain, the issue now is the determination of the second-order of approximation in the stress–strain relation. In fact, it can be seen that the Kelvin unit in Fig. 4 represents the interaction term between two components: the normal component and the shear component, as shown in Eq. (5.4).

As the example shown in Eqs. (6.2), (6.4)–(6.6) as well as in Figs. 5 and 6, one application of this theory is in the area of modeling asphalt concrete. In fact, using the model of generalized Maxwell elements to simulate the behavior of asphalt concrete has been reported by a number of researchers (Bouldin et al., 1993; Monismith et al., 1994). In those reports, the issue of why to employ a generalized Maxwell model and how many units of single Maxwell element are needed is determined empirically. The contact mechanism based theory presented in this article therefore provides a rational justification to use a generalized Maxwell model in representing asphalt concrete as well as how many units are needed in the representation.

Uniaxial viscoelastic modeling of a viscous matrix composite requires a huge effort, but multiaxial modeling is more challenging. In fact, very limited reports have been seen in the multiaxial analytical studies on viscous matrix composites. It appears that the derivation of Eqs. (3.2) and (3.4) are important that they may provide a platform upon which such studies can be pursued. Indeed, the confined creep case given in this article serves as an example of how this pursuit can be done. In addition, a quite comprehensive study including the particle angularity consideration has been carried out also on the same platform (Zhu and Nodes, 2000).

It appears that this contact mechanism based composite theory aims to address the issue of characterizing the behavior of viscous matrix composites. Many issues remain to be studied. For example, the matrix plays its role not only through the binder contact laws, but also has the role coming from its "non-contact" controlled portion, or pore pressure effect, which is not included in this study. As such, this theory may be applicable to the case when particles/fibers/inclusions are much more rigid than that of the matrix or the composites having some air voids like asphalt concrete. One way to incorporate the effect of "non-contact" portion of the matrix or pore pressure is to use a geometric equivalent approach in conjunction with the binder contact laws (Zhu et al., 1997b), and this incorporation on a Maxwell matrix composite will be reported separately.

References

Bathurst, R.J., Rothenburg, L., 1988. Micro-mechanical aspects of isotropic granular assemblies with line contact interactions. ASME J. Appl. Mech. 55, 17–23.

Bland, D.R., 1960. The Theory of Linear Viscoelasticity. Pergamon Press, Oxford.

Bouldin, M.G., Rowe, G.M., Sousa, J.B., Sharromk, M.J., 1993. Mix rheology-a tool for predicting the high temperature performance of hot mix asphalt. A.A.P.T. 63, 182–223.

Brown, S.F., Cooper, K.E., 1980. A fundamental study of the stress–strain characteristics of a bituminous materials. A.A.P.T. 49, 476–498.

Chen, C.-H., Cheng, C.-H., 1997. Micro-mechanical modeling of creep behavior in particle-reinforced silicone-rubber composites. J. Appl. Mech. 64, 781–786.

Chang, S.C., Misra, A., Sundaram, S.S., 1990. Micro-mechanical modeling of cemented sands under low amplitude oscillations. Geotechnique 40, 251–263.

Chang, S.C., Misra, A., 1990. Packing structure and mechanical properties of granulates. ASCE J. Engng. Mech. 116 (5), 1077–1093.

Chang, S.C., Ma, L., 1992. Elastic material constants for isotropic granular solids with particle rotation. Int. J. Solid Struct. 29, 1001–1018.

Chang, S.C., 1996. Moduli of granular materials with viscoelastic binders. Proceedings of ASME Mechanics and Materials Conference. Baltimore, MD.

Christoffersion, J., Mehrabadi, M.M., Nemat-Nasser, S., 1981. A micro-mechanical description of granular material behavior. J. Appl. Mech. 48, 339–344.

Cowin, S.C., 1985. The relationship between the elasticity tensor and the fabric tensor. Mech. Mater. 4, 137–147.

Finney, J.L., 1970. Random packings and structure of simple liquids. I. The geometry of random close packing. Proc. Royal Soc. Lond. A 319, 479–493.

Gladwell, G.M.L., 1980. Contact Problems in the Classical Theory of Elasticity. Alphen and den Rijn, Sijthoff and Noordhoff.

Hashin, Z., 1983. Analysis of composites materials – a survey. J. Appl. Mech. 50, 481–498.

Hopman, P.M., Pronk, A.M., Kunst, P.A.J.M., Molenaar, A.A.A., Molenarr, J.M.M., 1992. Application of the viscoelastic properties of asphalt concrete. 77th Int. Conf. Asphalt Pavements, pp. 73–89.

Jenkins, J.T., 1987. Volume change in small axi-symmetric deformations of a granular material. In: Satake, Jenkins (Eds.), Micro-mechanics of Granular Materials. Elsevier, Amsterdam, pp. 245–252.

Johnson, K.L., 1989. Contact Mechanics. Cambridge University Press, Cambridge.

Kanatana, K., 1984. Distribution of directional data and fabric tensor. Int. J. Engng. Sci. 22, 149–164.

Lee, X., Dass, W.C., 1993. The Effect of Tri-axial Loads on Packing Structures in a Granular Media with Asphalt Binder. Annual Technical Report for WL/FIVC. Applied Research Associates, Tyndall AFB, FL.

Lewandowski, L.H., Graham, R., Shoenberger, J., 1992. Physico-chemical and Rheological Properties of Microwave Recycled Asphalt Binders. Proceedings of the Materials Engineering Congress. ASME, New York, NY.

Monismith, C.L., et al., 1994. Permanent Deformation Response of Asphalt Aggregate Mixes. SHRP-A-415, Strategic Highway Research Program. NRC, Washington.

Oda, M., Nemat-Nasser, S., Meharabadi, M.M., 1982. A statistical study of fabric tensor in a random assembly of spherical granules. Int. J. Num. Anal. Meth. Geomech. 6, 77–85.

Ponte Castaneda, P., Willis, J.R., 1988. On the overall properties of nonlinear viscous composites. Proc. Royal Soc. Lond. A 416, 217–244.

Rothenberg, L., Selvadurai, A.P.S., 1981. Micro-mechanical definition of the cauchy stress tensor for particulate media. In: Selvadurai, A.P.S. (Ed.), Mechanics of Structured Media. Elsevier, Amsterdam, pp. 469–486.

Satake, M., 1982. Fabric tensor in granular materials. In: Vermeer, P.A., Luger, H.J. (Eds.), Proc. IUTAM Symp. on Deformation and Failure of Granular Materials. Delft, Netherlands, pp. 63–68.

Schapery, R.A., 1974. Viscoelastic behavior and analysis of composite materials. In: Sendeckyj, G.P. (Ed.), Mechanics of Composite Materials. Academic Press, New York.

Scherer, G.W., Rekhson, S.M., 1982. Viscoelastic/elastic composites. I. General theory. J. Am. Ceram. Soc. 65 (7), 352–360.

Shahinpoor, M., 1981. Statistical mechanical considerations on rolling bulk solids. Bulk Solids Handling 1, 31–36.

Trefethen, J.H., 1959. Geology for Engineers. Van Nostrand, Princeton, NJ.

Zabaras, N., Pervez, T., 1990. Viscous damping approximation of laminated anisotropic compoiste plates. Comput. Meth. Appl. Mech. Engng. 81, 291–316.

Zhu, H., Chang, C.S., Rish III, J.W., 1996a. Normal and tangential compliance for conforming binder contact. I: Elastic binder. Int. J. Solids Struct. 33, 4337–4349.

Zhu, H., Chang, C.S., Rish III, J.W., 1996b. Normal and tangential compliance for conforming binder contact. II. Visco-elastic binder. Int. J. Solids Struct. 33, 4351–4363.

Zhu, H., Dass, W.C., 1996c. Asphaltic Concrete Constitutive Behavior. WL/FIVC Report, Tyndall AFB, FL.

Zhu, H., Chang, C.S., Rish III, J.W., 1997a. Rolling compliance for elastic and viscoelastic conforming binder contact. Int. J. Solids Struct. 34, 4073–4086.

Zhu, H., Rish III, J.W., Dass, W.C., 1997b. A constitutive study of two-phase particulate materials. I. Elastic binder. Comput. Geotech. 20 (3), 303–323.

Zhu, H., 1998. Contact based asphalt concrete modeling. The 12th Engineering Mechanics Conference. San Diego, CA.

Zhu, H., Nodes, J.E., 2000. Contact based analysis of asphalt pavement with the effect of aggregate angularity. Mech. Mater. 32 (3), 193–202.